The WW1 Domain Enhances Autoinhibition in Smurf Ubiquitin Ligases

Natalia Ruetalo [1], Samira Anders [1], Carsten Stollmaier [1,2], Magnus Jäckl [1], Mira C. Schütz-Stoffregen [1,2], Nadine Stefan [2], Christine Wolf [1] and Silke Wiesner [1,2]

*1 - **Max Planck Institute for Developmental Biology,** Max-Planck-Ring 5, 72076 Tübingen, Germany*
*2 - **Institute of Biophysics and Physical Biochemistry,** University of Regensburg, Universitätsstr. 31, 93040 Regensburg, Germany*

***Correspondence to Silke Wiesner:** Institute of Biophysics and Physical Biochemistry, University of Regensburg, Universitätsstr. 31, 93040 Regensburg, Germany. silke.wiesner@ur.de*
https://doi.org/10.1016/j.jmb.2019.09.018
Edited by Titia Sixma

Abstract

Downregulation of ubiquitin (Ub) ligase activity prevents premature ubiquitination and is critical for cellular homeostasis. Nedd4 Ub ligases share a common domain architecture and yet are regulated in distinct ways through interactions of the catalytic HECT domain with the N-terminal C2 domain or the central WW domain region. Smurf1 and Smurf2 are two highly related Nedd4 ligases with ~70% overall sequence identity. Here, we show that the Smurf1 C2 domain interacts with the HECT domain and inhibits ligase activity *in trans*. However, in contrast to Smurf2, we find that full-length Smurf1 is a highly active Ub ligase, and we can attribute this striking difference in regulation to the lack of one WW domain (WW1) in Smurf1. Using NMR spectroscopy and biochemical assays, we identified the WW1 region as an additional inhibitory element in Smurf2 that cooperates with the C2 domain to enhance HECT domain binding and Smurf2 inhibition. Our work provides important insights into Smurf regulation and highlights that the activities of highly related proteins can be controlled in distinct ways.

Introduction

Ubiquitination is a posttranslational modification that controls a broad range of essential cellular processes in eukaryotes including endocytosis, protein interaction, localization and degradation, and DNA transcription and repair. The ubiquitination reaction is catalyzed by three enzymes that act in a consecutive manner [1]. An E1 enzyme activates ubiquitin (Ub) and transfers it to an E2 enzyme. Lastly, Ub is covalently linked to a substrate with the aid of a Ub ligase (E3 enzyme). Ub can be attached to proteins as monomer at a single or multiple Lys residues (monoubiquitination/multiubiquitination) or as a polymeric chain (polyubiquitination) that is linked *via* any of the seven Lys residues or the Ub N-terminus by the repeated action of the ubiquitination enzyme cassette [2]. The length and linkage of polyUb chains are largely determined by the E3 ligases and dictates the cellular fate of the modified target. Moreover, as E3 enzymes are the first in the reaction chain to interact with substrates, they play an important role in conferring specificity to the reaction. Not surprisingly, genetic alteration and deregulation of E3 enzymes are directly linked to a variety of diseases, including cancer [3].

A subfamily of E3 ligases contains a so-called HECT (Homologous to the E6AP Carboxyl Terminus) domain at the C-terminus that catalyzes Ub-substrate ligation in a two-step manner [4]. First, the HECT domain forms a thioester intermediate *via* its catalytic Cys with the C-terminus of Ub. Next, Ub is transferred from the HECT thioester to the ϵ-amino group of a Lys side chain in the substrate. Of note, many HECT domains depend on a noncovalent interaction with Ub to form polyUb chains [5–7]. Nedd4 family E3s are the largest class of HECT-type Ub ligases with nine members in humans (Nedd4, Nedd4L, WWP1, WWP2, Itch, Smurf1, Smurf2, HECW1, and HECW2) [8]. Nedd4 ligases target components of various signal transduction pathways that are crucial for developmental and carcinogenic

processes [9–14]. These enzymes share a conserved domain organization with an N-terminal C2 domain mediating membrane localization, two to four WW domains that contain two signature Trp residues and bind proline-rich substrates or adaptor proteins, and the C-terminal, catalytic HECT domain. In the absence of substrates or adaptor proteins, the catalytic activity of Nedd4-like family E3s is downregulated by intramolecular interactions that prevent premature auto- and substrate ubiquitination. In Nedd4 members, such as Smurf2, Nedd4, and Nedd4L [15–18], the N-terminal C2 domain interacts with the C-terminal HECT domain to inhibit ligase activity. In the Nedd4 members such as Itch, WWP1, and WWP2 instead, autoinhibition does not involve the C2 domain but is mediated by intramolecular interactions between the second WW domain, the WW2-3 linker, and the HECT domain [19–21]. In any case, these intramolecular interactions with the HECT domain prevent E2-E3 transthiolation and block noncovalent Ub binding.

Smurf1 and Smurf2 share 70% sequence identity for the full-length (FL) proteins with the major difference being the lack of the first WW domain in Smurf1 (Fig. 1a). Considering only the C2 and HECT domains, the level of sequence identity rises to even almost 90% suggesting that the autoinhibitory C2:HECT interaction should be conserved in Smurf1. However, reports on the catalytic activity in the literature disagree on whether Smurf1 activity is regulated [9,22–24]. Here, we investigated in detail the mechanism of Smurf ligase regulation. We found that the Smurf2 WW1 domain together with the C2-WW1 linker strongly enhances the C2:HECT interaction to effectively downregulate E3 ligase activity. Although Smurf1 and Smurf2 are highly related proteins, we find that, in contrast to Smurf2, Smurf1 is not inhibited by a C2:HECT interaction. We show here that this difference in regulation between Smurf1 and Smurf2 stems from the lack of the WW1 domain in Smurf1.

Results

The Smurf1 HECT domain interacts with the C2 domain *in trans*

To investigate whether the C2:HECT interaction is conserved between Smurf1 and Smurf2, we performed chemical shift perturbation (CSP) experiments with an AILMV (Ala β-, Ile δ_1-, Leu-$\delta_{1,2}$-, Met ϵ-, and Val $\gamma_{1,2}$-[^{1}H,^{13}C]-methyl-, but otherwise [^{2}H,^{12}C])-labeled Smurf1 HECT domain (Fig. 1b, Supplementary Fig. 1a). NMR spectroscopy is a highly sensitive tool to study biomolecular interactions as the resonance frequencies (chemical shifts) of the observed atomic nuclei depend on the local chemical environment. Ligand binding causes changes in the local chemical environment of those amino acids that are located in the binding pocket resulting in observable CSPs for those residues [25]. To examine whether the Smurf1 C2 domain interacts with the HECT domain, we recorded 2D ^{1}H,^{13}C correlation (HMQC) spectra of the AILMV-labeled HECT domain alone and in the presence of unlabeled Smurf1 C2 domain (Fig. 1b, Supplementary Fig. 1a). Comparison of these spectra revealed CSPs of more than 15 Hz for a number of methyl groups in the Smurf1 HECT domain. This demonstrates that the Smurf1 HECT domain interacts with the C2 domain.

To map the CSPs onto the structure of the Smurf1 HECT domain, we generated a homology model based on the sequence of the ~86% identical Smurf2 HECT domain (PDB ID: 1ZVD) [26] and assigned most of the Ile δ_1- and Met ϵ-methyl peaks in the IM (Ile δ_1- and Met ϵ-[^{1}H,^{13}C]-methyl-) HMQC spectrum of the Smurf1 HECT domain by point mutation of Ile and Met residues and comparison of the WT and mutant HMQC spectra. With this in hand, we can show that the Smurf1 C2 domain interacts with the HECT domain on a binding surface that is highly similar to Smurf2 (Fig. 1c, Supplementary Fig. 1b and c) [15,17]. To substantiate this result, we introduced a Y433M mutation in the Smurf1 HECT domain that is located within the C2 binding surface on the N-lobe (Fig. 1c) as an additional NMR reporter for C2 domain binding [17,27]. The additional peak resulting from the mutation could be easily identified by comparison of the mutant and WT HMQC spectra (Supplementary Fig. 1d). Indeed, addition of the Smurf1 C2 domain to this mutant altered the chemical shift of the Y433M methyl group. Otherwise, the CSPs for this mutant were similar to those observed in the WT Smurf1 HECT domain (Supplementary Fig. 1e). This result thus confirms the C2 binding surface mapped with the CSPs of the WT HECT domain.

To examine whether also the binding surface of the HECT domain on the C2 domain is conserved among Smurf1 and Smurf2, we recorded ^{1}H,^{15}N-correlation TROSY spectra of a partially deuterated, ^{15}N-labeled Smurf1 C2 domain in the absence and presence of increasing amounts of unlabeled HECT domain. We observed that a number of peaks in the Smurf1 C2 domain exhibited substantial CSPs (Fig. 1d). To map the HECT binding surface on the C2 domain, we assigned the backbone resonances of the Smurf1 C2 domain using standard triple resonance NMR experiments and visualized the observed CSPs on the crystal structure of the C2 domain (PDB ID: 3PYC) [22]. This revealed that also the HECT domain interacts with the C2 domain in Smurf1 using virtually the same binding surface as in Smurf2 (Fig. 1e) [15].

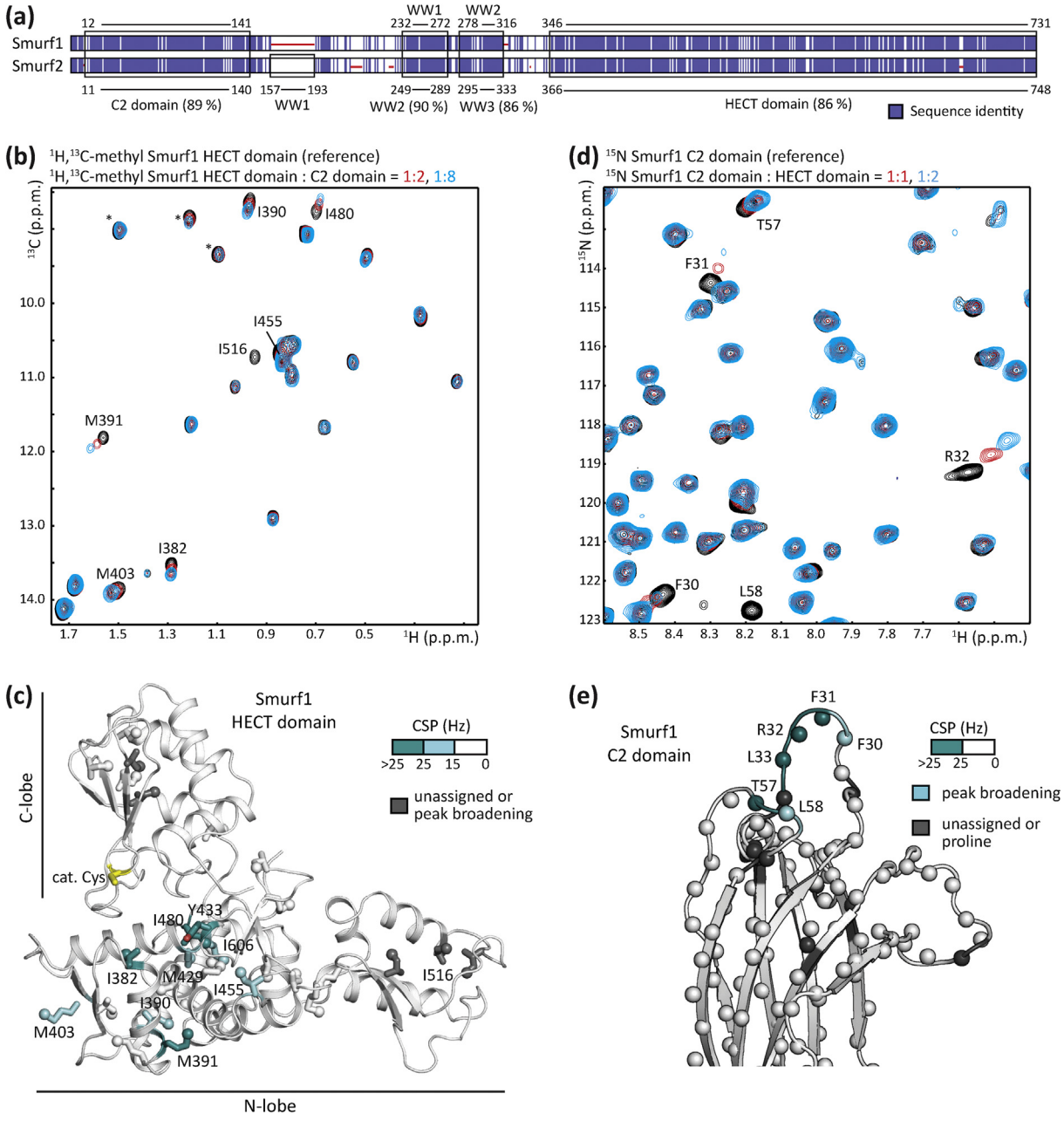

Fig. 1. The Smurf1 HECT domain interacts with the C2 domain on a surface that is conserved in Smurf2. (a) Sequence identity between Smurf1 and Smurf2. Identical residues are colored in blue. Alignment gaps are indicated with red lines. The regions comprising the C2, WW, and HECT domains are highlighted with black boxes, and the corresponding residue numbers are indicated. (b) Overlay of selected regions of $^{1}H,^{13}C$-methyl HMQC spectra of the AILMV-labeled Smurf1 HECT domain in the absence and presence of increasing amounts of unlabeled Smurf1 C2 domain. (c) Chemical shift mapping of the Smurf1 HECT:C2 interaction on a ribbon representation of a Smurf1 HECT homology model. Residues exhibiting CSPs >15 Hz at an eight-fold stoichiometric excess of C2 domain are color-coded as indicated. Ile and Met side chains are shown as sticks, while the isotope-labeled methyl carbons are shown as spheres. (d) Overlay of selected regions of $^{1}H,^{15}N$-TROSY spectra of the ^{15}N-labeled Smurf1 C2 domain in the absence and presence of increasing amounts of unlabeled Smurf1 HECT domain. (e) As c, but for HECT domain binding to the Smurf1 C2 domain. Residues exhibiting CSPs >15 Hz at a two-fold stoichiometric excess of HECT domain are color-coded as indicated. Nitrogen atoms are shown as spheres.

Finally, we compared the interactions of the C2 and HECT domains in Smurf1 and Smurf2 in a quantitative manner. To determine the dissociation constants (K_d values) for the Smurf1 and Smurf2 C2:HECT interactions, we performed 2D NMR line shape fitting analyses of methyl chemical shift titration experiments with the Smurf1 and Smurf2 HECT domains and the respective unlabeled C2 domains (Supplementary Table 1, Supplementary Fig. 2a–d) [28]. Both HECT domains interacted with their respective C2 domain with similarly weak affinities (347 ± 10 μM and 269 ± 6 μM for Smurf1 and Smurf2, respectively) (Table 1). Of note, the K_d value for Smurf2 lies in the same range as the previously reported K_d of 220 ± 6 μM for the C2:HECT interaction determined by fluorescence polarization [17]. In sum, these NMR binding studies show that the C2 domain of Smurf1 interacts with the HECT domain using the same binding interface and with similar affinity as in Smurf2.

Smurf1 contains a noncovalent Ub binding surface

Numerous HECT domains contain a noncovalent Ub binding surface (UBS) that promotes Ub chain elongation [5–7,29]. We therefore examined whether Smurf1 interacts with Ub in a noncovalent manner. Indeed, the IM-labeled Smurf1 HECT domain exhibited numerous CSPs on addition of unlabeled monomeric Ub, demonstrating that Smurf1 interacts with Ub in a noncovalent manner (Supplementary Fig. 3a). As in Smurf2, numerous residues, such as I382, I455, and I480, are involved in both Ub and C2 domain binding, demonstrating that these binding surfaces overlap on the Smurf1 HECT domain (Fig. 1b and c, Supplementary Fig. 1b and c, Supplementary Fig. 3a–d) [17]. To determine the K_d values for the Smurf1 and Smurf2 HECT:Ub interactions, we performed 2D NMR line shape fitting analyses of methyl chemical shift titration experiments with the Smurf1 and Smurf2 HECT domains and monomeric Ub (Supplementary Table S1, Supplementary Fig. 4a–d). Both HECT domains interacted with Ub with similar affinities (305 ± 16 μM and 396 ± 21 μM for Smurf1 and Smurf2, respectively) (Table 1). These values agree well with previous results on a number of HECT:Ub interactions [29]. In sum, as suggested by the high level of sequence identity of the Smurf1 and Smurf2 C2 and HECT domains, we find that the binding capabilities and affinities of the HECT domains towards monomeric Ub and the respective C2 domains are conserved between Smurf1 and Smurf2.

Table 1. Dissociation constants for the Smurf1 and Smurf2 HECT domains*.

Ligand	Smurf1	Smurf2
Ubiquitin	299 ± 17	393 ± 21
Smurf1/Smurf2 C2	347 ± 26	269 ± 20
Smurf2 C2-WW1	–	15 ± 4

*K_d values are given in μM and were determined by line shape fitting of NMR CSP experiments. Errors were estimated with bootstrapping statistics on 100 replica and assumed a 5% error in protein and ligand concentrations.

The C2 domain does not inhibit the activity of full-length Smurf1

In Smurf2, the C2 domain plays an important role in downregulating the activity of the HECT domain to prevent untimely target ubiquitination [15,17]. To investigate whether the C2 domain exerts a similar autoinhibitory effect on the HECT domain in Smurf1, we examined the autoubiquitination activities of recombinant WT Smurf1 and a Smurf1 variant lacking the C2 domain (ΔC2) and compared them to the corresponding Smurf2 proteins (Fig. 2a). Interestingly, we observed that the ΔC2 Smurf1 was comparable in activity to the FL protein (Fig. 2b), while deletion of the C2 domain in Smurf2 showed a dramatic increase in autoubiquitination activity for Smurf2 (Fig. 2c) as reported previously [15,17,22]. In contrast to Smurf2, the C2 domain thus does not inhibit autoubiquitination activity Smurf1 *in cis*, although it can interact weakly with the HECT domain *in trans* (Fig. 1b–e).

To examine whether the Smurf1 C2 domain has the potential to modulate HECT domain activity, we performed autoubiquitination assays with the Smurf1 HECT domain in the absence and presence of increasing amounts of C2 domain. Interestingly, although the C2 domain does not regulate the activity of FL Smurf1, the C2 domain can inhibit HECT domain activity *in trans* to a similar degree as in Smurf2 (Fig. 2d). This demonstrates that the Smurf1 C2 domain can interact and inhibit HECT domain activity *in trans* but cannot exert autoinhibition *in cis*. This result suggests that conformational restriction may prevent the C2 domain in Smurf1 from blocking HECT activity.

The WW1 domain and the linker region are involved in Smurf inhibition

Because the major differences between Smurf1 and Smurf2 lie in the region linking the C2 and HECT domains and in particular the lack of the WW1 domain in Smurf1 (Fig. 1a), the results of our ubiquitination assays suggest that these regions play a pivotal role in regulating Smurf activity. We therefore designed chimeric Smurf1 and Smurf2 proteins that contained the linker region of Smurf2 (Smurf1 FL: Smurf2 linker) or *vice versa* of Smurf1 (Smurf2 FL: Smurf1 linker) (Fig. 2a). Moreover, we introduced the Smurf2 WW1 domain in Smurf1

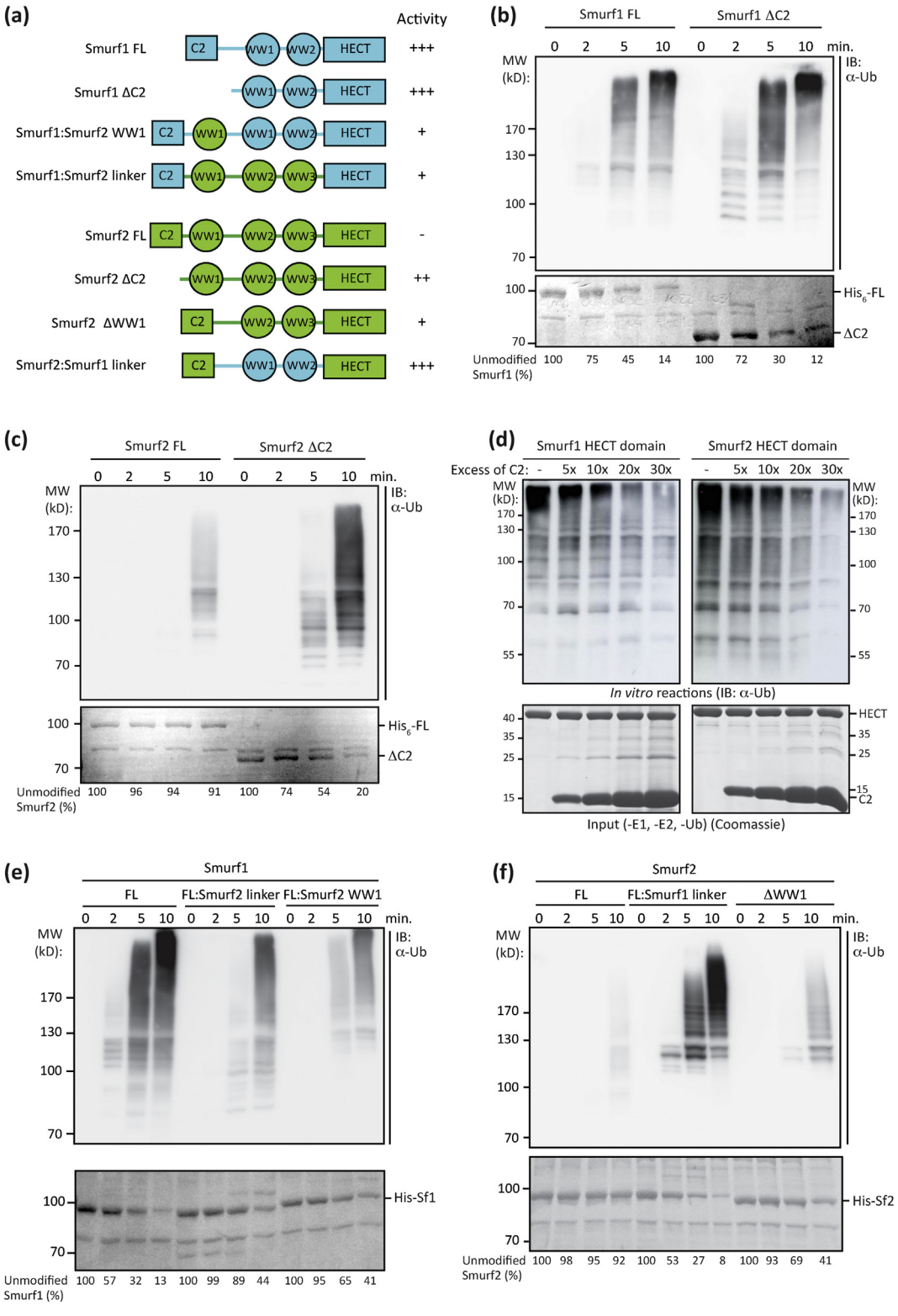
(a)
Activity
Smurf1 FL
Smurf1 ΔC2
Smurf1:Smurf2 WW1
Smurf1:Smurf2 linker
Smurf2 FL
Smurf2 ΔC2
Smurf2 ΔWW1
Smurf2:Smurf1 linker
C2
WW1
WW2
WW3
HECT
+++
+++
+
+
-
++
+
+++
(b)
Smurf1 FL
Smurf1 ΔC2
0 2 5 10 0 2 5 10 min.
MW (kD):
IB: α-Ub
170
130
100
70
His6-FL
ΔC2
Unmodified Smurf1 (%) 100 75 45 14 100 72 30 12
(c)
Smurf2 FL
Smurf2 ΔC2
0 2 5 10 0 2 5 10 min.
MW (kD):
IB: α-Ub
170
130
100
70
His6-FL
ΔC2
Unmodified Smurf2 (%) 100 96 94 91 100 74 54 20
(d)
Smurf1 HECT domain
Smurf2 HECT domain
Excess of C2: - 5x 10x 20x 30x - 5x 10x 20x 30x
MW (kD):
170
130
100
70
55
In vitro reactions (IB: α-Ub)
40
35
25
15
HECT
C2
Input (-E1, -E2, -Ub) (Coomassie)
(e)
Smurf1
FL
FL:Smurf2 linker
FL:Smurf2 WW1
0 2 5 10 0 2 5 10 0 2 5 10 min.
MW (kD):
IB: α-Ub
170
130
100
70
His-Sf1
Unmodified Smurf1 (%) 100 57 32 13 100 99 89 44 100 95 65 41
(f)
Smurf2
FL
FL:Smurf1 linker
ΔWW1
0 2 5 10 0 2 5 10 0 2 5 10 min.
MW (kD):
IB: α-Ub
170
130
100
70
His-Sf2
Unmodified Smurf2 (%) 100 98 95 92 100 53 27 8 100 93 69 41

(Smurf1 FL: Smurf2 WW1) and generated a Smurf2 variant lacking the WW1 domain (Smurf2 ΔWW1) (Fig. 2a).

Substitution of the Smurf1 linker with that of Smurf2 led to a significant loss in autoubiquitination activity as compared with WT Smurf1 and thus enabled Smurf1 autoinhibition (Fig. 2e). Accordingly, Smurf2 with a Smurf1 linker exhibited a considerably higher autoubiquitination activity than WT Smurf2, demonstrating that the Smurf1 linker region does not allow for efficient autoinhibition (Fig. 2f). Moreover, the presence of the Smurf2 WW1 domain enabled autoinhibition of FL Smurf1, albeit to a slightly lower degree than the entire Smurf2 linker region in Smurf1 (Fig. 2e). Accordingly, deletion of the WW1 domain led to Smurf2 activation, although the level of activation was lower than for Smurf2 carrying the Smurf1 WW linker region (Fig. 2f). This suggests that apart from the WW1 domain, other regions within the linker between the C2 and the HECT domain may play a role in Smurf autoinhibition.

Our assays thus demonstrate that the Smurf1 C2 domain is capable of binding and inhibiting the HECT domain *in trans*, but that the Smurf1 linker region and in particular the absence of the WW1 domain does not allow for the C2 and HECT interaction to occur in Smurf1 *in cis*.

The C2 domain interacts with the C2-WW1 linker

To gain insight into the role of the WW1 domain in Smurf autoinhibition, we sought to uncover intramolecular interactions in Smurf2 that involved the WW1 domain and its linker to the C2 domain. However, we have previously shown that the isolated Smurf2 WW1 domain does not interact with the HECT domain *in trans* [15]. Therefore, we examined whether the C2 domain can interact with WW1 domain *in trans*. To this end, we recorded 2D $^{1}H,^{15}N$-correlation spectra of the ^{15}N-labeled Smurf2 C2 domain in the absence and presence of increasing amounts of unlabeled Smurf2 WW1 domain. However, we did not detect chemical shift changes for the C2 domain on addition of the WW1 domain (Supplementary Fig. 5a). Similarly, we observed no CSPs in the Smurf2 WW1 domain when we compared the isolated WW1 domain (Smurf2 aa 157–197) with a WW1 domain preceded by the C2-WW1 linker (linker-WW1; Smurf2 aa 145–197) (Supplementary Fig. 5b and c) or to the WW1-WW2 module preceded by the C2-WW1 linker (linker-WW1-WW2 Y257W; Smurf2 Y257W aa 145–290) (Supplementary Fig. 5b and d). Of note, the WW2 domain included a substitution of Y257 to a Trp at the position of one of the signature Trp residues in WW domains to improve the stability of the domain. These NMR experiments demonstrated that the Smurf2 WW1 domain does not undergo intramolecular interactions with the C2-WW1 linker, the C-terminal linker, or the WW2 domain nor does it interact with the C2 domain *in trans*.

Next, we recorded a 2D $^{1}H,^{15}N$-correlation spectra of a ^{15}N-labeled Smurf2 C2-WW1 fragment (aa 10–197) and compared it with the isolated C2 domain and the linker-WW1 construct. Interestingly, this revealed numerous chemical shift changes for the C2-WW1 fragment (Fig. 3a). These CSPs thus reveal an intramolecular interaction within the C2-WW1 module of the Smurf2 ligase. To identify the residues involved in the intramolecular interaction, we assigned the backbone resonances of the C2-WW1 fragment using standard triple resonance NMR experiments. We found that the residues exhibiting CSPs in the C2-WW1 fragment compared with the isolated C2 domain or linker-WW1 construct mapped to the region close to the N- and C-terminus in the Smurf2 C2 domain and the C-terminal half of the C2-WW1 linker (Fig. 3b). We therefore conclude that the C2-WW1 linker folds back on the C2 domain *in cis*. Most notably, the region in the C2 domain that is affected by the presence of the C2-WW1 linker and the WW1 domain is directly adjacent to the HECT domain binding surface and thus may help to recruit the C2 domain to the HECT domain (Fig. 3b) [15].

The C2-WW1 linker and the WW1 domain enhance the C2:HECT interaction and Smurf2 autoinhibition

Having established that the C2 and C2-WW1 linker are structurally coupled in the Smurf2 C2-WW1 module, we examined next the effect of C2-

Fig. 2. The region connecting the C2 and HECT domains plays a role in Smurf autoinhibition. (a) Schematic representation of the Smurf1 and Smurf2 protein variants used for autoubiquitination assays. Autoubiquitination activity of the Smurf1 and Smurf2 proteins is indicated on the right-hand side based on the quantification of assays shown in (b–f). (b and c) *In vitro* ubiquitination assays using WT and ΔC2 Smurf1 (b) and Smurf2 (c) proteins. (d) Top: *In vitro* autoubiquitination of Smurf1 (left panel) and Smurf2 (right panel) HECT domains in the absence and presence of increasing amounts of the respective C2 domain as indicated. Bottom: Input samples showing equivalent HECT domain levels and increasing concentrations of the respective C2 domain. (e, f) *In vitro* ubiquitination assays using full-length (FL) and chimeric Smurf1 proteins (e) and FL, chimeric, and ΔWW1 Smurf2 proteins (f). All proteins were the bacterially expressed and purified. Reactions were stopped at the indicated time points. Reaction samples were separated by SDS-PAGE and autoubiquitination activity detected by immunoblotting (IB) with α-Ub antibody (top panels) or Coomassie (bottom panels) (b–c, e–f). Levels of unmodified E3 ligase at different time points relative to the starting point (t = 0 min; 100%) in the Coomassie images are indicated on the bottom.

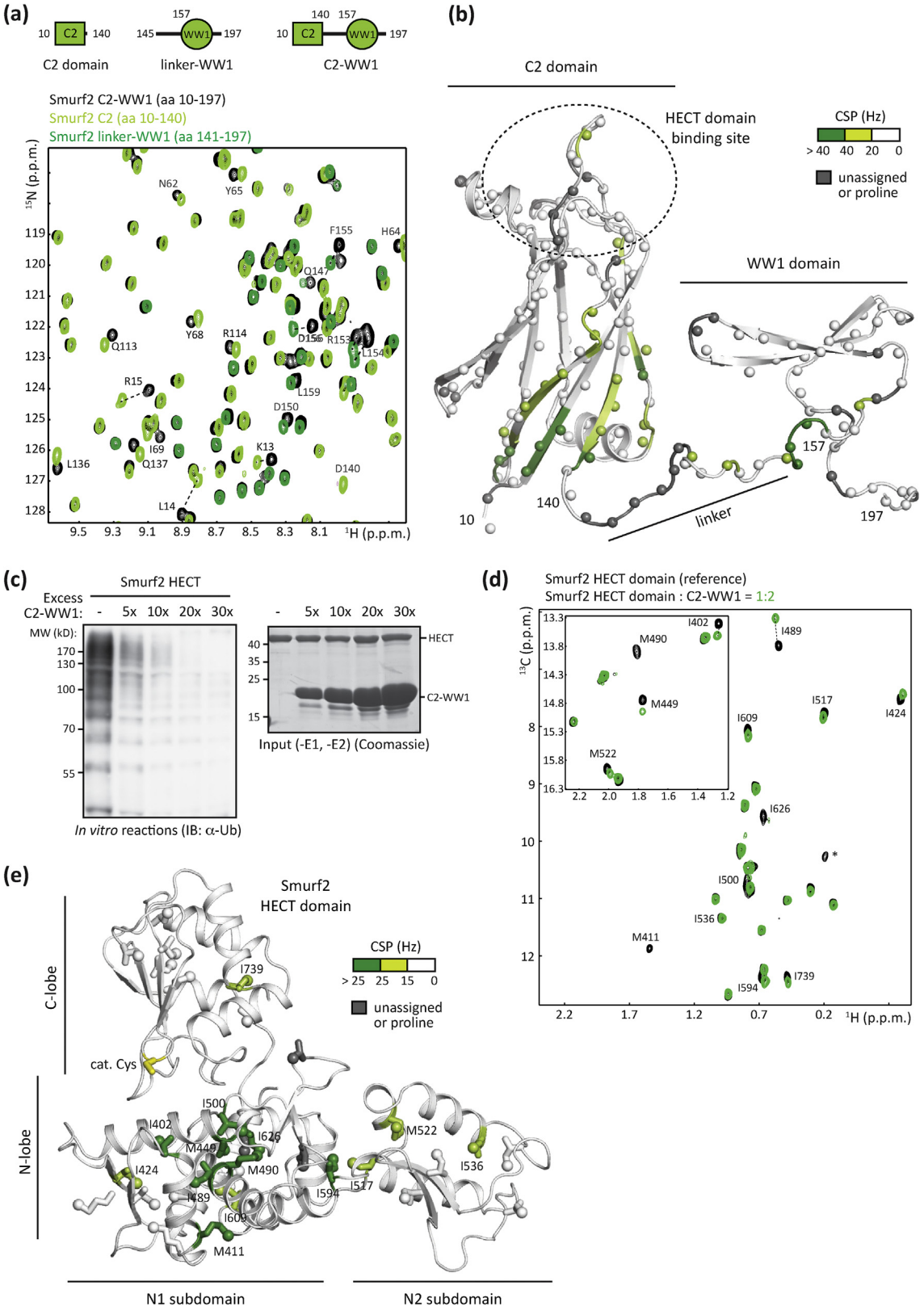
(a)
C2 domain
linker-WW1
C2-WW1
Smurf2 C2-WW1 (aa 10-197)
Smurf2 C2 (aa 10-140)
Smurf2 linker-WW1 (aa 141-197)
(b)
C2 domain
HECT domain binding site
CSP (Hz)
unassigned or proline
WW1 domain
linker
(c)
Smurf2 HECT
Excess C2-WW1:
MW (kD):
HECT
C2-WW1
Input (-E1, -E2) (Coomassie)
In vitro reactions (IB: α-Ub)
(d)
Smurf2 HECT domain (reference)
Smurf2 HECT domain : C2-WW1 = 1:2
(e)
Smurf2 HECT domain
C-lobe
N-lobe
cat. Cys
N1 subdomain
N2 subdomain

WW1 fragment on HECT domain activity. To this end, we performed autoubiquitination assays with the Smurf2 HECT domain in the absence and presence of increasing amounts of the C2-WW1 fragment. Although a large stoichiometric excess of the isolated C2 domain was required to inhibit the autoubiquitination activity of the Smurf2 HECT domain (Fig. 2d, right panel), the HECT domain was already strongly inhibited by a five-fold excess of the C2-WW1 fragment (Fig. 3c). This shows that the C2-WW1 fragment inhibits Smurf2 HECT domain activity more potently than the isolated C2 domain.

To exclude the possibility that the reduced HECT domain activity in the presence of the Smurf1 or Smurf2 C2 domain or the Smurf2 C2-WW1 fragment resulted from upstream effects on E1 or E2 activity, we performed E2 charging assays with UbcH7 in the absence of an E3 ligase. The presence of concentrations of the Smurf1 and Smurf2 C2 domain or the Smurf2 C2-WW1 fragment corresponding to a 30-fold excess in Figs. 2c and 3c had no effect on UbcH7 thioester formation (Supplementary Fig. 6a). This demonstrates that HECT domain inhibition by the C2 domains or the C2-WW1 fragment occurs on the level of the E3 ligase. Of note, this result is fully consistent with our previous observation that the C2 domain engaged in an intramolecular interaction that impairs thioester formation of the HECT domain [17].

Because the Smurf1 and Smurf2 C2 and HECT domains share high degrees of sequence identity (Fig. 1a), we also examined the cross-reactivity of the respective C2 and HECT domains of the other ligase. To this end, we performed autoubiquitination assays with the Smurf1 and Smurf2 HECT domains in the presence of the Smurf1 or Smurf2 C2 domain or the Smurf2 C2-WW1 fragment (Supplementary Fig. 6b and c). As expected based on the high degree of sequence identity, the Smurf1 HECT domain was not only inhibited by its own C2 domain but also by the Smurf2 C2 domain (Supplementary Fig. 6b). As in the case of Smurf2, the inhibitory effect of the C2 domain on the Smurf1 HECT domain was strongly enhanced when the Smurf2 C2 domain was fused to the WW1 domain (C2-WW1 fragment). Similar to Smurf1, the Smurf2 HECT domain was inhibited by both, its own C2 domain and the Smurf1 C2 domain (Supplementary Fig. 6c). Overall, these results are consistent with our studies of the chimeric Smurf1 proteins where the introduction of the Smurf2 C2-HECT linker sequence or the Smurf2 WW1 domain enabled autoinhibition of Smurf1 *in cis* (Fig. 2e).

To elucidate how the C2-WW1 linker and the WW1 domain modulate the C2:HECT interaction, we added the unlabeled C2-WW1 fragment to the IM-labeled Smurf2 HECT domain in a stepwise manner and compared the resulting $^{1}H,^{13}C$-methyl correlation spectra. In contrast to the isolated C2 domain, the C2-WW1 fragment induced CSPs in the HECT domain already at low stoichiometric amounts (Fig. 3d). Consistently, 2D NMR line shape fitting analysis showed that the C2-WW1 fragment greatly enhances the interaction with the HECT domain and increases the *in trans* affinity ~18-fold as compared with the isolated C2 domain (Table 1, Supplementary Table 1, Supplementary Fig. 7a–c). For many Ile and Met residues, such as I402, M411, I489, and I500, we noticed an almost linear progression of the CSPs on addition of the C2-WW1 fragment in comparison with the isolated C2 domain (Supplementary Fig. 1b, Fig. 3d and Supplementary Fig. 7a). This shows that apart from enhancing affinity, the binding mode of the C2 domain to these residues is not affected by the WW1 domain or the C2-WW1 linker. However, we also observed CSPs that deviated (I626) or were not present (I424, M449, M490, M522, M594, I609) for the isolated C2 domain. Mapping the observed CSPs on the Smurf2 HECT domain revealed that the presence of the C2-WW1 linker and the WW1 domain extends the binding surface towards the interface of the two subdomains that form the HECT domain N-lobe (Fig. 3e). Of note, this extension of the binding surface also results in an even more substantial overlap with the noncovalent UBS than for the isolated C2 domain (Fig. 3e, Supplementary Fig. 1c and Supplementary Fig. 3c). Taken together, our results show that the Smurf2 C2-WW1 linker and the WW1 domain enhance the affinity and inhibitory potential of the C2:HECT interaction by extension of the HECT domain binding surface.

Fig. 3. The Smurf2 C2-WW1 fragment enhances HECT domain binding and inhibition. (a) Chemical shift perturbation studies of the Smurf2 C2-WW1 fragment. Overlay of a representative region of the $^{1}H,^{15}N$-correlation spectra of ^{15}N-labeled Smurf2 constructs containing the WW1 domain as indicated. (b) Mapping of chemical shift perturbations in the C2-WW1 fragment using a homology model based on the NMR and crystal structures of the Smurf2 C2 domain and the YAP and Smurf1 WW1 domains (PDB IDs: 2LAY and 2LAZ). Residues exhibiting CSPs >20 Hz are color-coded as indicated. Nitrogen atoms are shown as spheres. (c) *In vitro* autoubiquitination of the Smurf2 (right panel) HECT domains in the absence and presence of increasing amounts of the C2-WW1 fragment as indicated, otherwise as Fig. 2(d). (d) Overlay of selected regions of $^{1}H,^{13}C$-methyl HMQC spectra of the IM-labeled Smurf2 HECT domain in the absence and presence of increasing amounts of the Smurf2 C2-WW1 fragment. (e) Chemical shift mapping on a ribbon representation of a Smurf2 HECT domain. Residues exhibiting CSPs >15 Hz at an eight-fold stoichiometric excess of the C2-WW1 fragment are color-coded as indicated.

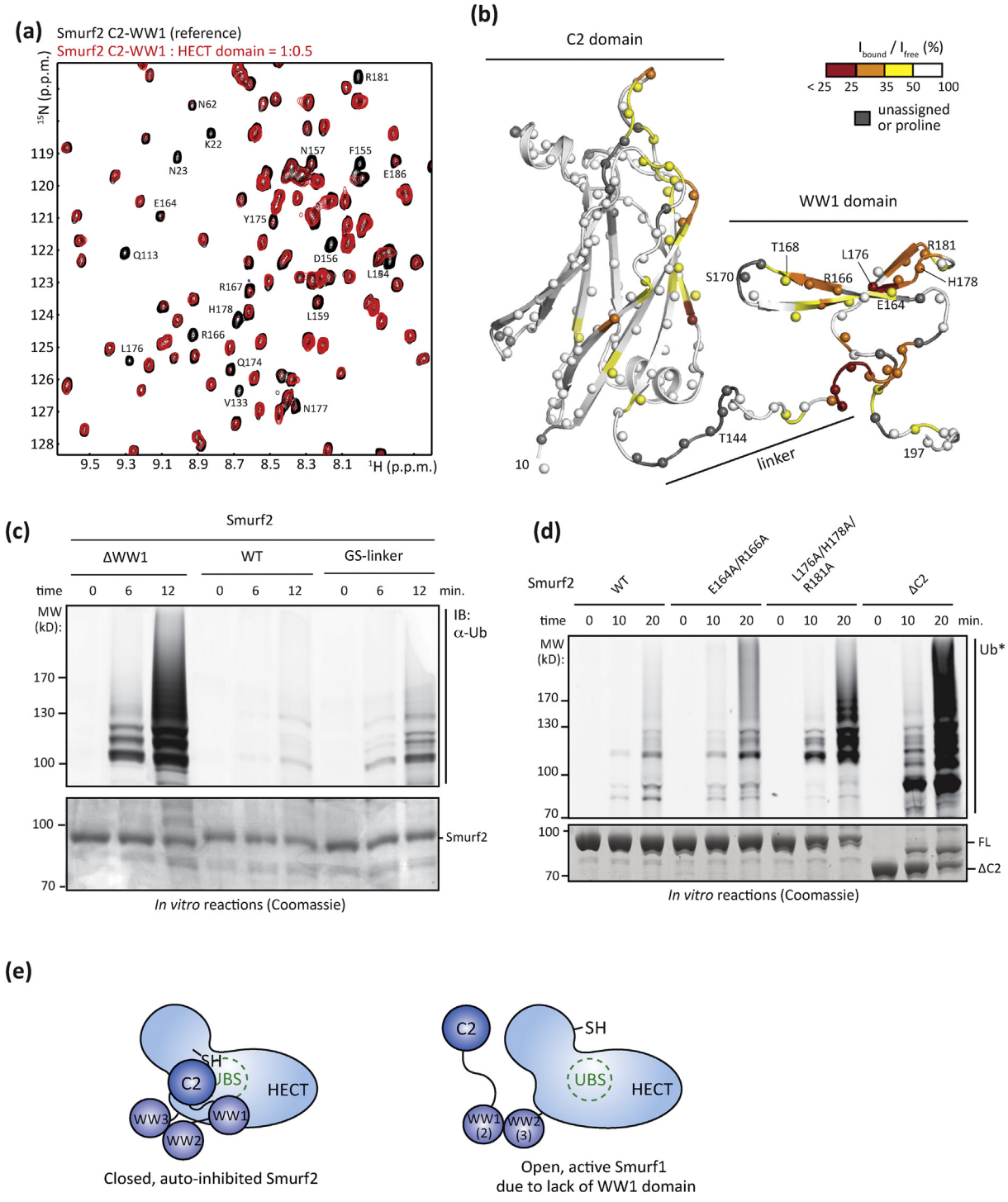

The Smurf2 HECT domain interacts with both the C2 domain and the WW1 region

To map the binding surface of the Smurf2 HECT domain on the C2-WW1 module, we added unlabeled HECT domain in a stepwise manner to the partially deuterated, ^{15}N-labeled C2-WW1 module. Comparison of the ^{1}H,^{15}N-correlation NMR spectra showed extensive line broadening in the C2-WW1 module already at low stoichiometric amounts of the HECT domain as expected for a binding affinity in the lower micromolar range and the formation of a >50 kD protein complex (Fig. 4a). Mapping of the CSPs on a structural model of the C2-WW1 module exhibited not only the already known HECT domain binding surface on the C2

domain but also the region surrounding the N- and C-terminus of the C2 domain, the C2-WW1 linker, and the WW1 domain (Fig. 4b). These findings suggest that the C2-WW1 linker and the WW1 domain preassemble with the C2 domain to enlarge the interaction surface with the HECT domain and to enhance the binding affinity in comparison with the isolated C2 or WW1 domain.

Mutation of the C2-WW1 linker and the WW1 domain enhance Smurf2 activity

To investigate the importance of the C2-WW1 linker in the context of the Smurf2 ligase, we replaced the linker with a sequence consisting of glycine and serine residues (Smurf2 GS-linker) and assessed the catalytic activity of this Smurf2 variant by comparing its autoubiquitination capabilities to those of FL and ΔWW1 Smurf2. We found that substitution of the linker sequence indeed enhanced Smurf2 activity in comparison to the WT protein, albeit not to the same degree as the deletion of the WW1 domain (Fig. 4c). We thus conclude that the C2-WW1 linker contributes to Smurf2 autoinhibition but that its mutation is not sufficient to fully release the C2 and WW1 domains from the HECT domain.

Moreover, to examine the importance of the WW1 domain in Smurf2 inhibition, we introduced site-specific mutations in the Smurf2 WW1 domain in the context of the FL protein. Guided by the NMR binding studies (Fig. 4a and b), we designed a double and a triple Smurf2 mutant (E164A/R166A and L176A/H178A/R181A) where we substituted WW1 residues that showed CSPs on HECT domain interaction (Fig. 4b). Both, the double and the triple mutant, displayed elevated activity compared with the WT Smurf2 protein in autoubiquitination assays (Fig. 4c). Taken together, these assays show that mutations in the HECT domain binding surface of the WW1 domain and mutation of the C2-WW1 linker both interfere with the C2-WW1:HECT interaction and thereby relieve Smurf2 autoinhibition.

In sum, our NMR and biochemical analyses demonstrate that the C2 and WW1 domain in Smurf2 form a supramodule where the C2-WW1 linker directly interacts with the C2 domain and together with the WW1 domain significantly enhances the interaction with HECT domain. This enhanced interaction in turn results in more efficient inhibition of HECT domain activity. In contrast, the lack of the WW1 domain in Smurf1 may prevent the C2 domain from binding the HECT domain tightly enough to inhibit ligase activity providing a rationale for the differential regulation of these two highly related enzymes (Fig. 4e).

Discussion

Most eukaryotic proteins consist of domains that mediate specific interactions and/or catalytic activity [30]. Although protein domains are in principle structurally and functionally independent, their activities are often modulated through intramolecular interactions with other domains or linker regions in so-called supramodules [31,32]. However, how linker regions and the formation of supramodules regulate protein function and the activity of catalytic domains is still poorly understood, limiting the possibilities of predicting regulatory mechanisms based on domain composition and sequence similarity.

For numerous Nedd4 Ub ligases, the mechanisms underlying autoinhibition have been investigated [15,17,19–21]. Surprisingly, despite their common domain architecture and high levels of sequence conservation within the C2, WW, and HECT domains, the mode of autoinhibition seems to be distinct for the individual Nedd4 family members. In a subset of Nedd4 ligases, the N-terminal C2 domain interacts directly with the catalytic HECT domain, while in Itch, WWP1, and WWP2, the WW2 domain and the WW2–WW3 linker interact with the HECT domain to inhibit ubiquitination activity.

Fig. 4. Both the Smurf2 C2-WW1 linker and the WW1 domain interact with the HECT domain. (a) Overlay of selected regions of $^{1}H,^{15}N$-TROSY spectra of the ^{15}N-labeled Smurf2 C2-WW1 fragment in the absence and presence of increasing amounts of unlabeled Smurf2 HECT domain. (b) Mapping of the chemical shift perturbations induced by the HECT domain on the ribbon representation of C2-WW1 fragment. Nitrogen atoms are shown as spheres. Residues exhibiting CSPs ($I_{bound}/I_{free} > 50\%$) at a stoichiometric ratio of 1:0.5 are color-coded as indicated. Mutation sites in the WW1 domain (E164/R166 and L176/H178/R181) assayed in (d) are highlighted. Reported phosphorylation sites (T144, T168, S170) are indicated. (c) *In vitro* ubiquitination assays using WT and ΔWW1 Smurf2 and a Smurf2 variant where the C2-WW1 linker was substituted with Gly and Ser residues (GS-linker), otherwise as Fig. 2b. (d) *In vitro* ubiquitination assays using WT and ΔC2 Smurf2 and Smurf2 variants with mutated WW1 binding surfaces (E164A/R166A and L176A/H178A/R181A). Autoubiquitination activity was detected by fluorescence imaging. The use of fluorescently labeled Ub is indicated with Ub*, otherwise as Fig. 2b. (e) A schematic representation of the conformations of the full-length Smurf proteins is shown. Binding of the C2 domain together with the WW1 domain and the C2-WW1 linker to the HECT domain in Smurf2 enables a closed, autoinhibited conformation where the C2-WW1 binding surface overlaps with the Ub binding surface (UBS) (upper panel). The lack of the WW1 domain in Smurf1 prevents the C2 domain from interacting with the HECT domain *in cis* resulting in an open a constitutively active full-length Smurf1 enzyme (lower panel). The numbers in parentheses of the Smurf1 WW domains indicates the respective equivalent WW domain in Smurf2.

Here, we have investigated the regulation of the highly related Ub ligases Smurf1 and Smurf2. Surprisingly, we find that despite sharing ~70% sequence identity, Smurf1 is not downregulated by a C2:HECT interaction, although the Smurf1 C2 domain can interact with the HECT domain and inhibit its activity *in trans*. We can attribute this differential regulation to the presence of an additional WW domain (WW1) in Smurf2 and show that the C2-WW1 linker and the WW1 domain strongly enhance the C2:HECT interaction and consequently the inhibition of the HECT domain. This identifies the C2-WW1 linker and the WW1 domain as regions mediating Smurf autoinhibition in addition to the C2 domain. Interestingly, we identified three phosphorylation sites in the region comprising the Smurf2 C2-WW1 linker and the WW1 domain (T144, T168, and S170) that are conserved among humans, mice, and rats [33]. At least two of these sites (T168 and S170) lie in direct vicinity to the WW1:HECT interaction surface (Fig. 4b) and thus may play a role in regulating Smurf2 autoinhibition.

Consistent with the C2-WW1 region playing a role in Smurf2 autoinhibition, we find that recombinant FL Smurf1 that naturally lacks the WW1 domain is a constitutively active enzyme *in vitro*. Although a C2-mediated inhibition of Smurf1 has been reported in a previous study [23], our results fully agree with at least three other studies that find Smurf1 not being regulated by a C2:HECT interaction [9,22,24]. In any case, it is unknown whether Smurf1 is indeed a constitutively active ligase under endogenous expression levels in cells. Because Smurf1 plays important roles in key developmental processes, it seems unlikely that Smurf1 activity would not be regulated *in vivo*. Mechanisms of regulation that are obscured under *in vitro* or overexpression conditions include posttranslational modification Smurf1 or the interaction with adaptor proteins that may inhibit Smurf1 activity in cells. Moreover, target-regulated expression or differential activity depending on the cellular localization of Smurf1 could also prevent premature target ubiquitination. In fact, the substrate specificities of Smurf ligases have been linked to both posttranslational modifications [14,34,35] and cellular localization [22].

Lastly, given the high level of sequence identity between Smurf1 and Smurf2, the result that these enzymes are regulated differently is surprising. This study thus emphasizes the importance of detailed mechanistic studies to decipher the molecular basis of ligase activity. As Nedd4 family members are important regulators of developmental and carcinogenic processes, the detailed studies of the catalytic mechanisms and differential regulation of these enzymes as presented here have direct implications not only for understanding their function but also for the design of novel ligase-selective therapeutics.

Materials and Methods

Constructs and reagents

Human wild-type Smurf2 (Sf2) (aa 1−748), ΔC2 (aa 145−748), and the HECT domain (aa 366−748) were described previously [15]. A codon-optimized gene fragment of the C2 domain (aa 10−140) was purchased from ThermoFisher and cloned into a modified pETM-60 vector encoding an additional N-terminal His_6-tag. Sf2 ΔWW1 (aa 1−162, 186−754 Sf2) and Sf2 GS-linker (aa 1−146 Sf2, SGGSG, 156−754 Sf2) were generated from FL Smurf2 using the QuikChange Site-Directed Mutagenesis protocol (Stratagene). The Sf2 C2-WW1 fragment (aa 10−197), WW1 domain (aa 157−197), linker-WW1 (aa 145−197), and linker-WW1-2 Y257W (WW1-2) (aa 145−290; Y257W) were cloned in pETM-41 vectors by restriction-free cloning [36]. A cDNA clone encoding human Smurf1 (Sf1) was obtained from ImaGenes. The regions comprising FL Sf1 (aa 1−731; isoform 2), ΔC2 (aa 146−731), and the HECT domain (aa 345−731) were cloned into pProExHTb vectors, while the C2 domain was cloned into a pETZ2-1A vector amplified from a codon-optimized gene fragment obtained from ThermoFisher. All chimeric proteins were generated by restriction-free cloning [36]: Sf1 FL: Sf2 linker (aa 1−142 Sf1, 141−365 Sf2, 344−731 Sf1), Sf2 FL: Sf1 linker (aa 1−141 Sf2, 142−344 Sf1, 366−748 Sf2), and Sf1 FL: Sf2 WW1 (aa 1−158 Sf1, 158−193 Sf2, 164−731 Sf1).

All point mutations were introduced using the QuikChange Site-Directed Mutagenesis Protocol (Stratagene). All clones were verified by DNA sequencing. Bacterial plasmids were transformed into chemically competent *Escherichia*(*E.*) *coli* DH5α (ThermoFisher) or BL21-CodonPlus (DE3) RIL cells (Stratagene). Antibodies were α-Ub (P4D1; Santa Cruz) and HRP-coupled mouse IgG secondary antibody (ThermoScientific).

Protein expression and purification

All recombinant proteins were expressed in *E. coli* BL21-CodonPlus (DE3) RIL cells (Stratagene). Cultures were grown at 37 °C in Luria broth medium for unlabeled proteins or in H_2O- or D_2O-based M9 minimal medium for ^{15}N-, $^{15}N,^{13}C$-, and $^{1}H,^{13}C$-methyl-labeled proteins as described [15]. Cells were induced with 1 mM IPTG and grown overnight (~16 h) at 18 °C for unlabeled proteins or at 25 °C for isotope-labeled proteins. Cells were harvested by centrifugation and lysed by sonication on ice. Cell debris was removed by centrifugation. Soluble recombinant proteins in the supernatants were purified by Ni-affinity. His-tagged N-terminal solubility tags (NusA, MBP, or Z domain) were cleaved with His-tagged TEV protease and removed together

with the protease *via* Ni-affinity and/or size exclusion chromatography if required. For proteins expressed from pETM-11 or pProExHTb vectors, the His-tag was only removed for the HECT domains or if indicated. Proteins were buffer exchanged either into NMR buffer (20 mM Na phosphate pH 6.5 or 7.5, 150 mM NaCl, 1 mM DTT containing 10% or 99% D_2O for methyl-labeled proteins) or gel filtration buffer for biochemical assays (50 mM Tris pH 7.5, 200 mM NaCl, 2.5% glycerol, 1 mM DTT).

NMR

For HECT domains, CSP experiments were performed by recording 2D $^{1}H,^{13}C$-methyl-HMQC spectra of 40 μM AILMV- or IM-labeled HECT domains before and after addition of unlabeled C2 domain, C2-WW1 fragment, or monomeric Ub at 30 °C. For the Smurf2 WW1 domain, the C2-WW1, and the linker-WW1-WW2 constructs, 2D $^{1}H,^{15}N$-TROSY spectrum of 100 μM ^{15}N-labeled sample was acquired at 25 °C. For the Smurf1 and Smurf2 C2 domains, 2D $^{1}H,^{15}N$-HSQC spectra of 100 μM ^{15}N-labeled C2 domain in the absence or presence of unlabeled Smurf1 HECT domain or Smurf2 WW1 domain were recorded at 25 °C.

For resonance assignment of the Smurf1 methyl groups, in total, 29 individual point mutants (I375V, I382L, I390V, M391V, M393V, M403V, M429V, I444V, M446V, I449L, I455V, I469V, M470V, I480V, I497V, I516V, I521V, I539V, M571V, I574V, I589V, I605V, I606V, I612V, I632V, I683V, I686V, I703V, and I705V) of the Smurf1 HECT domain were generated. 2D $^{1}H,^{13}C$-methyl-TROSY spectra of ~40 μM IM-labeled mutant Smurf1 HECT domains were recorded at 30 °C and compared with the WT spectrum. For backbone resonance assignment of the Smurf1 C2 domain, the Smurf2 WW1 domain, and the Smurf2 C2-WW1 construct, CBCANH, CBCA(CO)NH, (H)CC(CO)NH-TOCSY, and ^{15}N-edited 3D NOESY experiments were recorded at 25 °C.

NMR spectra of HECT domains and the Smurf2 WW modules were collected on an 800 MHz Bruker Avance-III spectrometer. All triple resonance experiments were acquired on a 600 MHz Bruker Avance-III spectrometer. Both spectrometers were equipped with room temperature probe heads. All NMR data were acquired using TOPSPIN 2.1 (Bruker Biospin GmbH), processed with the NMRPipe/NMRDraw program suite [37], analyzed with XEASY [38] or NMRFAM-Sparky [39], and visualized with NMRView (oneMoon Scientific).

Chemical shift perturbation and K_d determination

CSPs were analyzed using Sparky [39] and calculated as average changes in peak positions ($\Delta\delta_{Av} = [(\delta(^{1}H))^2 + (\delta(^{15}N \text{ or } ^{13}C))^2]^{1/2}$) in Hz or in cases of line broadening as loss in intensity (I_{bound}/I_{free}) on ligand binding by dividing the peak intensities of the titration spectrum (I_{bound}) with those of the free protein (I_{free}). Dissociation constants were calculated by 2D NMR line shape fitting from $^{1}H,^{13}C$-methyl-HMQC spectra using TITAN according to developer's instructions and online documentation [28]. Spectra were acquired with 1024 and 120 points in the ^{1}H and ^{13}C dimensions, respectively, and processed with exponential window functions with a line broadening of 4 Hz and 8 Hz. Spectra were zero-filled to 4096 and 480 points in the ^{1}H and ^{13}C dimensions, respectively. Errors were estimated with bootstrapping statistics on 100 replicas and assumed a 5% error in both protein and ligand concentrations. Titration points and peaks used for K_d fitting are summarized in Supplementary Table 1.

Structure modeling and visualization

Homology models of the Smuf1 HECT domain and the Smurf2 C2-WW1 fragment were generated using HHPred/Modeller [40,41] based on the structure of the Smurf2 HECT domain (1ZVD) [26] that shares 86% sequence identity with the Smurf1 HECT domain (Fig. 1a), the Smurf2 C2 domain (2JQZ) [15], and the YAP and Smurf1 WW1 domains in complex with Smad1 peptides (2LAY and 2LAZ) [42]. All structural representations were prepared with PyMOL (The PyMOL Molecular Graphics System, Version 1.7.4 Schrödinger, LLC).

Ubiquitination assays

In vitro ubiquitination assays were carried out as described [17]. In brief, 25 μL reactions were performed at 25 °C in ubiquitination buffer (25 mM Tris-HCl pH 7.5, 5 mM $MgCl_2$, 100 mM NaCl, 0.2 mM DTT, 2.5 mM ATP) using purified enzymes (0.6 μM E1, 90 μM UbcH7 [E2], 2 μM E3 [Smurf1 or Smurf2]) and 65 μM unlabeled or fluorescently labeled Ub (Ub*) [43]. Reactions were stopped at indicated time points by addition of 10 μL 3× Laemmli buffer containing 100 mM DTT. Samples were loaded for SDS-PAGE on 8% acrylamide gels. Detection was performed by fluorescence imaging (Ub*) or immunoblotting (IB) as indicated. SDS gels or PVDF membranes were stained with Coomassie where indicated. Levels of unmodified ligase were quantified using Fiji/ImageJ [44]. The intensities of unmodified E3 protein bands were measured at the indicated time points and normalized to the zero time points (t = 0 min; 100%).

For C2 and C2-WW1 competition assays, ubiquitination assays were performed as described above. The reaction mixtures contained 2.5 μM Smurf1 or Smurf2 HECT domain in the absence or presence of increasing amounts of the respective C2 domain or

the C2-WW1 fragment (12.5, 25, 50, or 75 μM). Samples were incubated for 20 min and loaded on 16% acrylamide gels for SDS-PAGE and IB or fluorescence imaging. Input samples contained the reaction mixture but not E1 and E2 and were detected by Coomassie staining.

E2 charging assays were performed in the same way as the competition assays. The reaction mixtures contained 75 μM Smurf1 or Smurf2 C2 domain or Smurf2 C2-WW1 but did not include an E3 enzyme. Reactions were stopped at indicated time points by addition of 10 μL 3× Laemmli buffer with or without DTT. Proteins were visualized after SDS-PAGE by fluorescence imaging and Coomassie staining.

Accession numbers

Backbone resonance assignments for the Smurf1 C2 domain, the Smurf2 WW1 domain, and the Smurf2 C2-WW1 construct and the $^{1}H,^{13}C$-methyl assignments of the Smurf1 HECT domain have been deposited in the BioMagResBank under accession numbers 50023, 50021, 50022, and 50024.

Acknowledgments

S.W. acknowledges support from the Max Planck Society, Germany, and a Marie Curie Reintegration grant by the Marie Skłodowska–Curie Actions Research Fellowship Programme of the European Commission (PIRG04-GA-2008-239418 UBLIGATION). We would like to acknowledge Timo Reitinger (University of Regensburg, Germany) for help with cloning and protein purification, Vincent Truffault (MPI for Developmental Biology, Tübingen, Germany) for support and maintenance of the NMR spectrometers and Fulvia Bono (MPI for Developmental Biology, Tübingen, Germany) for helpful discussions and suggestions.

Authors' Contributions

N.R., S.A., C.S., M.J., M.C.S.-S., N.S., and C.W. cloned and purified protein construct; N.R., S.A., M.J., C.W., and S.W. conducted and analyzed NMR experiments; N.R., C.S., and N.S. performed all activity assays; N.R. and S.W. conceived the idea for the project, designed experiments, and analyzed the results; S.W. wrote the paper with the help of N.R. All authors reviewed the results and approved the manuscript.

Competing Interests

The authors declare no conflict of interest.

Appendix A. Supplementary data

Supplementary data to this article can be found online at https://doi.org/10.1016/j.jmb.2019.09.018.

Received 27 May 2019;
Received in revised form 23 September 2019;
Accepted 26 September 2019
Available online 16 October 2019

Keywords:
Smurf HECT ligases;
WW domain;
Auto-inhibition;
Ubiquitination;
Methyl NMR spectroscopy

References

[1] A. Hershko, A. Ciechanover, The ubiquitin system, Annu. Rev. Biochem. 67 (1998) 425–479.
[2] N. Zheng, N. Shabek, Ubiquitin ligases: structure, function, and regulation, Annu. Rev. Biochem. 86 (2017) 129–157.
[3] D. Popovic, D. Vucic, I. Dikic, Ubiquitination in disease pathogenesis and treatment, Nat. Med. 20 (2014) 1242–1253.
[4] J.M. Huibregtse, M. Scheffner, S. Beaudenon, P.M. Howley, A family of proteins structurally and functionally related to the E6-AP ubiquitin-protein ligase, Proc. Natl. Acad. Sci. U. S. A. 92 (1995) 5249.
[5] E. Maspero, S. Mari, E. Valentini, A. Musacchio, A. Fish, S. Pasqualato, et al., Structure of the HECT:ubiquitin complex and its role in ubiquitin chain elongation, EMBO Rep. 12 (2011) 342–349.
[6] H.C. Kim, A.M. Steffen, M.L. Oldham, J. Chen, J.M. Huibregtse, Structure and function of a HECT domain ubiquitin-binding site, EMBO Rep. 12 (2011) 334–341.
[7] A.A. Ogunjimi, S. Wiesner, D.J. Briant, X. Varelas, F. Sicheri, J. Forman-Kay, et al., The ubiquitin binding region of the Smurf HECT domain facilitates polyubiquitylation and binding of ubiquitylated substrates, J. Biol. Chem. 285 (2010) 6308–6315.
[8] D. Rotin, S. Kumar, Physiological functions of the HECT family of ubiquitin ligases, Nat. Rev. Mol. Cell Biol. 10 (2009) 398–409.
[9] T. Mund, M. Graeb, J. Mieszczanek, M. Gammons, H.R. Pelham, M. Bienz, Disinhibition of the HECT E3 ubiquitin ligase WWP2 by polymerized dishevelled, Open Biol 5 (2015) 150185.
[10] S. Yue, L.Y. Tang, Y. Tang, Y. Tang, Q.H. Shen, J. Ding, et al., Requirement of Smurf-mediated endocytosis of Patched1 in sonic hedgehog signal reception, eLife 3 (2014).
[11] M.B. Wilkin, A.M. Carbery, M. Fostier, H. Aslam, S.L. Mazaleyrat, J. Higgs, et al., Regulation of notch endosomal sorting and signaling by Drosophila Nedd4 family proteins, Curr. Biol. 14 (2004) 2237–2244.
[12] H. Zhu, P. Kavsak, S. Abdollah, J.L. Wrana, G.H. Thomsen, A SMAD ubiquitin ligase targets the BMP pathway and affects embryonic pattern formation, Nature 400 (1999) 687–693.

[13] S.J. Bae, M. Kim, S.H. Kim, Y.E. Kwon, J.H. Lee, J. Kim, et al., NEDD4 controls intestinal stem cell homeostasis by regulating the Hippo signalling pathway, Nat. Commun. 6 (2015) 6314.
[14] M. Narimatsu, R. Bose, M. Pye, L. Zhang, B. Miller, P. Ching, et al., Regulation of planar cell polarity by Smurf ubiquitin ligases, Cell 137 (2009) 295–307.
[15] S. Wiesner, A.A. Ogunjimi, H.-R. Wang, D. Rotin, F. Sicheri, J.L. Wrana, et al., Autoinhibition of the HECT-type ubiquitin ligase Smurf2 through its C2 domain, Cell 130 (2007) 651–662.
[16] T. Mund, H.R. Pelham, Control of the activity of WW-HECT domain E3 ubiquitin ligases by NDFIP proteins, EMBO Rep. 10 (2009) 501–507.
[17] S. Mari, N. Ruetalo, E. Maspero, M.C. Stoffregen, S. Pasqualato, S. Polo, et al., Structural and functional framework for the autoinhibition of Nedd4-family ubiquitin ligases, Structure 22 (2014) 1639–1649.
[18] J. Wang, Q. Peng, Q. Lin, C. Childress, D. Carey, W. Yang, Calcium activates Nedd4 E3 ubiquitin ligases by releasing the C2 domain-mediated auto-inhibition, J. Biol. Chem. 285 (2010) 12279–12288.
[19] C. Riling, H. Kamadurai, S. Kumar, C.E. O'Leary, K.P. Wu, E.E. Manion, et al., Itch WW domains inhibit its E3 ubiquitin ligase activity by blocking E2-E3 ligase trans-thiolation, J. Biol. Chem. 290 (2015) 23875–23887.
[20] Z. Chen, H. Jiang, W. Xu, X. Li, D.R. Dempsey, X. Zhang, et al., A Tunable Brake for HECT ubiquitin ligases, Mol. Cell 66 (2017) 345–357 e6.
[21] K. Zhu, Z. Shan, X. Chen, Y. Cai, L. Cui, W. Yao, et al., Allosteric auto-inhibition and activation of the Nedd4 family E3 ligase itch, EMBO Rep. 18 (2017) 1618–1630.
[22] K. Lu, P. Li, M. Zhang, G. Xing, X. Li, W. Zhou, et al., Pivotal role of the C2 domain of the Smurf1 ubiquitin ligase in substrate selection, J. Biol. Chem. 286 (2011) 16861–16870.
[23] L. Wan, W. Zou, D. Gao, H. Inuzuka, H. Fukushima, A.H. Berg, et al., Cdh1 regulates osteoblast function through an APC/C-independent modulation of Smurf1, Mol. Cell 44 (2011) 721–733.
[24] T. Courivaud, N. Ferrand, A. Elkhattouti, S. Kumar, L. Levy, O. Ferrigno, et al., Functional characterization of a WWP1/Tiul1 Tumor-derived mutant reveals a paradigm of its constitutive activation in human cancer, J. Biol. Chem. 290 (2015) 21007–21018.
[25] S. Wiesner, R. Sprangers, Methyl groups as NMR probes for biomolecular interactions, Curr. Opin. Struct. Biol. 35 (2015) 60–67.
[26] A.A. Ogunjimi, D.J. Briant, N. Pece-Barbara, C. Le Roy, G.M. Di Guglielmo, P. Kavsak, et al., Regulation of Smurf2 ubiquitin ligase activity by anchoring the E2 to the HECT domain, Mol. Cell 19 (2005) 297–308.
[27] M. Stoffregen, M. Schwer, F. Renschler, S. Wiesner, Methionine scanning as an NMR tool for detecting and analyzing biomolecular interaction surfaces, Structure 20 (2012) 573–581.
[28] C.A. Waudby, A. Ramos, L.D. Cabrita, J. Christodoulou, Two-dimensional NMR lineshape analysis, Sci. Rep. 6 (2016) 24826.
[29] W. Zhang, K.P. Wu, M.A. Sartori, H.B. Kamadurai, A. Ordureau, C. Jiang, et al., System-wide modulation of HECT E3 ligases with selective ubiquitin variant probes, Mol. Cell 62 (2016) 121–136.
[30] T. Pawson, Protein modules and signalling networks, Nature 373 (1995) 573–580.
[31] Y. Li, Z. Wei, Y. Yan, Q. Wan, Q. Du, M. Zhang, Structure of crumbs tail in complex with the PALS1 PDZ-SH3-GK tandem reveals a highly specific assembly mechanism for the apical crumbs complex, Proc. Natl. Acad. Sci. U. S. A. 111 (2014) 17444–17449.
[32] N.H. Shah, J.F. Amacher, L.M. Nocka, J. Kuriyan, The Src module: an ancient scaffold in the evolution of cytoplasmic tyrosine kinases, Crit. Rev. Biochem. Mol. Biol. 53 (2018) 535–563.
[33] P.V. Hornbeck, I. Chabra, J.M. Kornhauser, E. Skrzypek, B. Zhang, PhosphoSite: a bioinformatics resource dedicated to physiological protein phosphorylation, Proteomics 4 (2004) 1551–1561.
[34] P.L. Cheng, H. Lu, M. Shelly, H. Gao, M.M. Poo, Phosphorylation of E3 ligase Smurf1 switches its substrate preference in support of axon development, Neuron 69 (2011) 231–243.
[35] B. Ozdamar, R. Bose, M. Barrios-Rodiles, H.R. Wang, Y. Zhang, J.L. Wrana, Regulation of the polarity protein Par6 by TGFbeta receptors controls epithelial cell plasticity, Science 307 (2005) 1603–1609.
[36] S.R. Bond, C.C. Naus, RF-Cloning.org: an online tool for the design of restriction-free cloning projects, Nucleic Acids Res. 40 (2012) W209–W213.
[37] F. Delaglio, S. Grzesiek, G.W. Vuister, G. Zhu, J. Pfeifer, A. Bax, NMRPipe: a multidimensional spectral processing system based on UNIX pipes, J. Biomol. NMR 6 (1995) 277–293.
[38] C. Bartels, T.H. Xia, M. Billeter, P. Guntert, K. Wuthrich, The program XEASY for computer-supported NMR spectral analysis of biological macromolecules, J. Biomol. NMR 6 (1995) 1–10.
[39] W. Lee, M. Tonelli, J.L. Markley, NMRFAM-SPARKY: enhanced software for biomolecular NMR spectroscopy, Bioinformatics 31 (2015) 1325–1327.
[40] V. Alva, S.Z. Nam, J. Soding, A.N. Lupas, The MPI bioinformatics Toolkit as an integrative platform for advanced protein sequence and structure analysis, Nucleic Acids Res. 44 (2016) W410–W415.
[41] B. Webb, A. Sali, Protein structure modeling with MODELLER, Methods Mol. Biol. 1654 (2017) 39–54.
[42] E. Aragon, N. Goerner, A.I. Zaromytidou, Q. Xi, A. Escobedo, J. Massague, et al., A Smad action turnover switch operated by WW domain readers of a phosphoserine code, Genes Dev. 25 (2011) 1275–1288.
[43] M. Jäckl, C. Stollmaier, T. Strohäker, K. Hyz, E. Maspero, S. Polo, S. Wiesner, β-Sheet Augmentation Is a Conserved Mechanism of Priming HECT E3 Ligases for Ubiquitin Ligation. J. Mol. Biol. 430 (2018) 3218–3233.
[44] J. Schindelin, I. Arganda-Carreras, E. Frise, V. Kaynig, M. Longair, T. Pietzsch, et al., Fiji: an open-source platform for biological-image analysis, Nat. Methods 9 (2012) 676–682.